Journal Pre-proofs

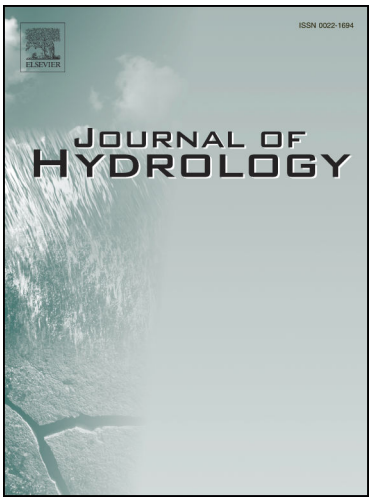

Research papers

Hydrologic performance of grass swales in cold maritime climates: Impacts of frost, rain-on-snow and snow cover on flow and volume reduction

Tarek Zaqout, Hrund Ólöf Andradóttir

PII: S0022-1694(21)00206-7
DOI: https://doi.org/10.1016/j.jhydrol.2021.126159
Reference: HYDROL 126159

To appear in: *Journal of Hydrology*

Received Date: 30 October 2020
Revised Date: 9 February 2021
Accepted Date: 3 March 2021

Please cite this article as: Zaqout, T., Ólöf Andradóttir, H., Hydrologic performance of grass swales in cold maritime climates: Impacts of frost, rain-on-snow and snow cover on flow and volume reduction, *Journal of Hydrology* (2021), doi: https://doi.org/10.1016/j.jhydrol.2021.126159

Hydrologic performance of grass swales in cold maritime climates: Impacts of frost, rain-on-snow and snow cover on flow and volume reduction

Tarek Zaqout *, Hrund Ólöf Andradóttir

Faculty of Civil and Environmental Engineering, University of Iceland; Hjarðarhagi 6, 107 Reykjavik, Iceland;

tarek@hi.is, hrund@hi.is

* Corresponding author

Abstract

Sustainable urban drainage solutions (SuDS) are a diverse set of design options that mitigate floods and improve water quality. Grass swales are the sole component of SuDS that transports runoff over long distances to downstream recipients. A deeper understanding of the performance of grass swales in different winter conditions is important in order for cities to achieve a greater climate resiliency. The goal of this study was to assess the impacts of frequent rain-on-snow, and freeze-thaw cycles on the hydrologic performance of grass swales. A total of 63 field synthetic runoff experiments were performed in a 5.8 m long section of a grass swale in the Urriðaholt neighborhood, Gardabaer, Iceland over 18 months. A three-fold reduction in peak flow attenuation was observed in winter (avg. 13%) compared to summer (avg. 38%) for hydraulic loadings ranging between 19 to 131 cm/h. The reduction in the performance of the swale was primarily due to frost formation and secondarily due to snow. The frequent rainfall, snowmelt, and rain-on-snow events elevated the soil water content and rendered the swale media susceptible to frost formation. The formation of pore ice within the 5 cm

soil horizon led to a considerable reduction in soil porosity, which negatively affected the infiltration capacity, and shortened runoff lag times. Snow affected the performance by concentrating the flow in narrow channels, which reduced the effective area of infiltration, but also led to longer lag times and stored a portion of the runoff water within its pack. Despite the deterioration in the swale efficiency in winter, infiltration was observed in all synthetic runoff experiments, indicating that frost was either porous/granular, or heterogeneous in nature. The swale served its purpose to moderately reduce runoff peaks and volumes, especially for small and medium events. This research highlights the importance of effectively draining infiltration-based systems in cold climates to avoid the adverse effects of low temperatures.

Keywords: Grass swales, SuDS, Infiltration into frozen soils, Runoff on snow, Flow reduction, Drainage capacity.

1. Introduction

Urban densification, together with intensifying weather, are exerting pressure on the conventional stormwater management systems and thus leading to more frequent and serious urban floods (Davis et al., 2012; Dietz & Clausen, 2008; Khan et al., 2012). Sustainable urban Drainage Systems (SuDS) have been increasingly implemented as a low impact stormwater control measure (SCM) to reduce runoff quantity and improve its quality. SuDS involve a wide range of design options with the goal of disposing stormwater in local waterways and mimicking the natural hydrological cycle. Vegetated swales are the sole component of SuDS elements that is intended to convey runoff across a watershed, while also performing the traditional functions of infiltrating and storing runoff, recharging the water table, and trapping and removing sediments and pollutants (Ahmed et al., 2015; Gavrić et al., 2019; Rujner et al., 2018). Hence, swales are paramount in making urban areas more climate resilient. The hydrological performance of swales during real and simulated runoff events has been extensively studied in temperate climates (e.g., Abu-Zreig et al., 2004; Davis et al., 2012; Deletic & Fletcher, 2006; García-Serrana et al., 2017; Liu et al., 2016; Lucke et al., 2014; Rujner et al., 2018; Shafique et al., 2018). A swale's hydrological and hydraulic performance is observed through reduced runoff volumes and delayed peak flows. The infiltration capacity of swales and their ability to store water are largely dependent on soil physical properties, type of soil, soil hydraulic conductivity, initial moisture content, and the area of the vegetated surface. A swale's infiltration capacity is also linked to the magnitude and intensity of runoff events (Davis et al., 2012). Bed slopes and surface roughness

provided by vegetation also affect flow retardation and infiltration (Monrabal-Martinez et al., 2018; Rujner et al., 2018).

SuDS water treatment and flood mitigation performance are negatively affected by winter conditions (Roseen et al., 2009). Even in highly conductive soils, such as sandy loam (Monrabal-Martinez et al., 2018; Paus et al., 2015), frost can clog the pores and form ice lenses that impair infiltration. In this regard, frost type is more important than frost depth (Muthanna et al., 2008). Frost type is largely governed by the pre-freezing soil water content, as saturated soils are more prone to concrete frost formation that blocks infiltration. Unsaturated or dry soil conditions promote granular and porous frost, both of which favor infiltration (Fach et al., 2011; LeFevre et al., 2009; Muthanna et al., 2008; Orradottir et al., 2008). A good drainage capacity is paramount to avoid high water content buildup, which has been shown to enhance volume reduction and prevent frost formation (LeFevre et al., 2009; Monrabal-Martinez et al., 2018; Muthanna et al., 2008).

Another factor known to promote urban flooding is the presence of snow. Winter runoff events become more voluminous with the addition of meltwater (Moghadas et al., 2018; Valeo & Ho, 2004). Being snow accumulation or snow deposit areas, SuDS are more prone to snowmelt compared to other vegetated urban areas (Bäckström & Viklander, 2000; Valeo & Ho, 2004). This is particularly true for swales, which are designed as channels or depressions and often located next to roads. When subjected to repeated freeze-thaw and rain-on-snow (RoS) cycles, icy layers form within the snowpack that prevent infiltration and can contribute to instantaneous runoff generation during RoS and snowmelt events (Caraco & Claytor, 1997; Garvelmann et al., 2015;

Muthanna et al., 2008). Moreover, the lack of a continuous insulating snow cover, as common in inland regions, renders coastal soils more susceptible to repeated meltwater infiltration and re-freezing contributing to impermeable frost formation (Orradottir et al., 2008). The repeated freezing and thawing processes can, however, alter soil aggregate stability and pore continuity, resulting in the creation of preferential flow paths that may promote infiltration (Flerchinger et al., 2013; Paus et al., 2015).

Little research exists on the performance of SuDS during frost, snow, and RoS in cold maritime climates. The most detailed studies on SuDS winter performance focused on bioretention cells, which exhibited anything from complete capture of runoff volumes to impeded infiltration in the presence of surface frost (e.g., Paus et al., 2015; Blecken et al., 2007; Khan et al., 2012; LeFevre et al., 2009; Muthanna et al., 2008). The different responses were attributed to a combination of soil hydraulic conductivity and drainage capacity, and the nature of runoff, whether it involves RoS or snowmelt (Muthanna et al. 2008; Paus et al. 2015). The effects of frost formation, soil saturation, and, more importantly, infiltration capacity were not investigated in depth in these studies. In addition, the number of snowmelt and RoS events were too few to clearly distinguish them from pure rainfall events. The studied bioretention cells included an underdrain and thick vegetation (e.g., Khan et al., 2012; Muthanna et al., 2008; Paus et al., 2015), which help keep the soil dry, prevent frost formation, and enhance infiltration. This differs from the relatively uniform vegetation cover and dense roots system of grass swales, many of which do not include an underdrain. Results from the bioretention cells may, therefore, not translate to grass swales. Particularly, the bioretention cells' good overall performance in cold climates might be attributed to the

fact that they are designed to temporarily pond water (Woods Ballard et al., 2015), which ultimately infiltrates the soil through preferential flow paths and macropores despite the frozen filter media (Khan et al., 2012). Swales, however, are designed to convey water and have a much shorter residence time. Very limited documentation exists on the functioning of grass swales in cold climates, especially during frozen conditions and in the presence of snow.

To the authors' knowledge, a systematic study of the hydrologic performance of SuDS during frost, snow, and, more specifically, RoS has not been conducted. RoS and intermittent mid-winter snowmelt events that have historically been associated with cold maritime climates are now becoming more common and severe in various regions around the globe due to climate change (Dong & Menzel, 2020; Garvelmann et al., 2015). Frequent RoS and freeze-thaw cycles were found to be responsible for 83% of water related insurance claims in the capital of Iceland (Arnardóttir, 2020). It is therefore essential to better understand the complex interconnections between soil, snow, and frost in order to successfully integrate such systems in stormwater management strategies. The goal of this study, therefore, was to assess the performance of grass swales under frost, RoS, and snow conditions. 63 synthetic runoff experiments were conducted in a swale segment in a residential neighborhood from March 2019 to August 2020. The tests were conducted during a range of snow, frost, and low temperatures to allow comparisons between these different conditions.

2. Methods

2.1. Site description

Urridaholt is the first BREEAM (Building Research Establishment's Environmental Assessment Method) certified neighborhood in Iceland, which is sited on a hill in the Gardabaer municipality in the greater capital area (64° 4’18.46” N, 21° 54’37.11” W). The drainage network was designed to protect the water level and quality in the shallow 13-ha Urridavatn pond at the bottom of the catchment (Fig. 1). For that purpose, excess runoff that infiltrates into roadside swales, detention ponds, and front loans from the 10-ha catchment area is conveyed via underdrains and discharged as concentrated flows into a network of swales that lead towards the pond. The main swale extends from the top of the hill towards the lake, with mild sloping sections separated by check dams to attenuate the flow.

The swale was constructed in 2009, using local material without specific layering. The vegetation cover is 1 to 3 cm tall grass during winter and 5 to 10 cm in summer. The 45 cm swale media is comprised of mostly sand mixed with a small portion of gravel and fine sediments (Table 1), based on three samples from the top 30 cm horizon extracted in accordance with ASTM D7263 (ASTM, 2009) and analyzed in accordance with ASTM D6913 (ASTM, 2017) and USDA Soil Textural Classification (USDA, 1987). Three replicas were tested in the laboratory to determine the soil’s saturated hydraulic conductivity, K_{sat}, using a constant head permeability test in accordance with ASTM D2434 (ASTM, 2019). Intact soil samples were also collected.

149 Soil porosity and bulk density were then determined. The bed below the 45 cm soil
150 horizon consists of hard compacted clay lying on top of rock.
151

152 2.2. Experimental design

153 Synthetic runoff experiments were conducted in a 5.8 m long, trapezoidal swale
154 section with an average bed width of 2 m (Fig. 2) and longitudinal slope of 3.3%. The
155 side slopes ranged between 10 to 22%. A portable water delivery system, consisting of
156 a 1 m^3 water tank filled with water from a nearby fire hydrant, was designated to feed
157 the swale with simulated runoff inflows. Using a submersible pump, water was pumped
158 from the tank into a smaller upstream reservoir equipped with a 45º V-notch weir using
159 a submersible pump. Flow rates were adjusted by ensuring a constant water level in the
160 delivery tank and increasing or decreasing the number of pumps used for the
161 corresponding inflow rate. The overflow from the inflow weir box was distributed evenly
162 over of the bottom channel of the swale. The overland flow that did not infiltrate from the
163 swale (runoff) was collected from a plastic sheet inserted 20 centimeters beyond the turf
164 and was directed into the outflow weir box at the end of the swale section.
165 The runoff simulations were performed using constant inflow rates of 0.2 l/s (very
166 low), 0.65-1.0 l/s (low), 2.0 l/s (medium), and 4.2 l/s (high flow) for a duration of 20-30
167 minutes. The experimental runs were timed to target a range of surface and soil
168 conditions (Table 2). On each day, two to three experiments were conducted
169 consecutively with a 30 to 45-minute resting period in between to limit the duration of
170 the experiment, and to allow for all water in the depressions to infiltrate. A total of 63
171 runoff simulations were conducted in the period from March 2019 to August 2020 to

capture data for winter, the transitional period of thawing during spring, and warm summers when swales are biologically active.

2.3. Data collection

Long-term monitoring. The swale was equipped with five water content reflectometers that continuously measured volumetric water content and temperature (type CS650, Campbell Scientific, Inc., accuracy ±1%, Caldwell, Bongiovanni, Cosh, Halley, & Young, 2018). The water content reflectometers were installed at the middle of the lower swale section at depths of 5, 15, 25, 35, and 45 cm placed horizontally from top to bottom; the top is located just below the 5 cm thick turf layer (Fig. 2; Right). Readings were logged using a data logger (Campbell Scientific Inc.) every 1 minute. A soil-specific calibration was conducted in the laboratory, and a linear user-defined calibration equation was derived (R^2 = 0.99) (Campbell Scientific Inc., 2012).

Ten-minute weather, air temperature, and rainfall data were collected from a weather station erected in February 2019 and operated by the Icelandic Meteorological Office [IMO] on behalf of the Gardabaer municipality (IMO, 2020a). The station is located approx. 70 m downstream from the study swale (Fig. 1). Daily snow depth was obtained from the Reykjavik No.1 weather station (64º07.648', 21º54.166'; IMO, 2020b). The station is situated on a hilltop vegetated with grass (52 m a.s.l) at a central location in the city at a distance of approximately 6 km from the study site.

Pre/post surface cover conditions. In winter, snow cover depth and density were measured in the field prior to the experimental runs by extracting three snow cores from the side of the swale or the unused swale section. The average and standard deviation

of the three measurements were determined and the overall accuracy of the snow depth measurements was determined to be 3-16% and for the snow density 1-13%. Snow height was re-estimated at the end of the consecutive experiments if the snow cover was not fully melted during the experiments. The presence of frost was investigated based on surface hardness, by inserting a blade into the soil and by visually noting the presence of ice crystals in the uppermost 5 cm (Orradottir et al., 2008). Surface and water temperature were measured using a handheld thermometer prior to the experimental run.

Hydrological monitoring during experiments: The inflow and outflow tanks were instrumented with pressure transducers (type Solinst 3001 Levelogger, accuracy ± 0.05% of full range). Water level measured at 10-s intervals was then converted into flow rates using the Kindsvater–Shen equation for V-notch weirs (Shen, 1981). For the accuracy of the pressure transducer sensors (±3 mm) and the ranges of water level measurements, the overall accuracy of the flow measurements was estimated to be 1-6 %. For quality purposes, inflow and outflow rates were also measured manually using a graduated cylinder as well as a stopwatch in case of a calibration error or a sensor malfunction. The effective width and depth of surface flow was measured manually at 1-m intervals along the length of the swale segment. In the presence of snow, the area of snow being wetted was also measured manually at 1-m intervals.

2.4. Derived data

2.4.1. Hydrological performance metrics

For each synthetic experiment, the volume of total flow, the lag time between inflow and outflow, and the peak flow reduction were determined from hydrographs, as shown on Fig. 3a. The relative peak flow reduction or flow attenuation was defined as the difference between the steady state inflow and outflow:

$$\Delta Q_{pk\,rel} = \frac{Q_{in} - Q_{out}}{Q_{in}} \quad (1)$$

The water balance components in the swale, and due to the limited duration of the experimental runs, can be defined as $V_{in} = V_{inf} + V_{out}$. The inflow volume includes the melt volume from the snowpack, V_{melt}. The total inflow and outflow volumes can be determined by integrating the flow rates, and the relative infiltrated volume or volume reduction, can be defined as

$$\Delta V_{inf\,rel} = \frac{V_{in} - V_{out}}{V_{in}} \quad (2)$$

The lag time between the inflow and outflow, T_{lag}, is defined as the difference between the centroids of the two hydrographs as shown in Fig. 3a (Viessman & Lewis, 2002).

233 The fourth and final hydrological performance metric is the ratio of the wetted area
234 to the total swale area. In absence of snow, the wetted width increases with the
235 increase in inflow rate. In winter, however, snow cover can influence the effective area
236 for infiltration, as schematically explained in Fig. 3. At the beginning of an event (Fig.
237 3a), runoff water wets the snow until it reaches its maximum water-holding capacity
238 (wetting phase). This also marks the start of the process of wetting the soil (Fig. 3b and
239 c). Afterwards, the runoff forms a flow path in the snowpack and the flow is
240 concentrated within the resulting channel until it reaches the outflow end of the swale
241 (runoff phase). At this time the soil reaches its maximum saturation and steady-state
242 conditions prevail (Fig. 3b). When the inflow to the swale ceases, runoff continues for an
243 average of 10 minutes. At this stage, the remaining runoff water exits the swale in the
244 form of outflow and infiltrates the ground and the drainage phase starts. Drainage is a
245 slower process, as can be seen in Fig. 3b as saturation remains almost unchanged
246 following the end of the experiment for a longer period before drainage commences.
247 The fraction of the wetted area or the areal efficiency, *AE*, was estimated as the
248 ratio of average overland flow width, W_{flow}, and total swale width, W_{total}, taken as the
249 width of the bottom channel of the swale.
250

$$AE = \frac{W_{flow}}{W_{total}} \quad (3)$$

251

252 *2.4.2. Soil performance metrics*

253 The swale was divided volumetrically into 5 sections according to the depth at which
254 each sensor was located with a volume of V_i (m^3) and the total moisture content in the
255 swale at time *t*, $V_w(t)$ (m^3), was estimated as
256

$$V_w(t) = \sum_{i=1}^{5} \theta_i(t) V_i \quad (4)$$

257

258 where θ_i is the measured water content by sensor *i* at time *t*.
259 The degree of saturation in the swale at time *t*, *DS(t)* (%) was then estimated as
260 the ratio of the total moisture volume in the swale V_w at time *t* and saturated moisture
261 volume V_{sat} as
262

$$DS(t) = \frac{V_w(t)}{V_{sat}} \times 100 \quad (5)$$

263

264 The saturated moisture volume was determined as the sum of the available pore
265 volume in each layer based on the measured porosity. Furthermore, an event maximum
266 surface porosity was estimated as the ratio of the measured maximum water content at
267 the surface during the experiment and the measured porosity in the same layer, i.e.
268

$$Event \max surface\ porosity = \frac{\max\left[\theta_{i=1}(t)\right]}{Porosity_{measured}} \times 100 \quad (6)$$

269

270 The drainage capacity, *DC*, of the swale was estimated as the reduction in the degree
271 of saturation 24 h after the last event on each experimental day (ΔDS_{24}). Drainage can
272 take from one to two days, depending on the swale's *DC*. A 24-hour drainage period
273 was chosen due to the frequent rain and snowmelt that could lead to the rewetting of
274 the soil before reaching field capacity.

275

276 2.5. Statistical analyses

277 Winter was defined as the four-month period when air temperature started to
278 descend below 0 °C (November) and lasted until the end of March. Spring was defined
279 as the two months of April and May. Surface conditions during winter and spring were
280 classified into four groups: Neutral, N when neither snow nor frost was present. Frozen,
281 F, if frost was detected with hardness test manually before the experimental run when
282 surface; or alternatively, when soil temperature was below or close to zero, and/or when
283 volumetric water content at 5 cm or deeper remained constant during the synthetic
284 experiment. Snow, S, and Snow on frost, SoF, when snow was present at the surface.
285 Warm conditions, W, indicated the three summer months (June to August), during which
286 surface or soil temperature exceeded 10 °C. The differences between the means of the
287 different surface conditions and seasons for each performance metric were analyzed

using analysis of variance (ANOVA), and multiple comparisons were performed using student's t test. Statistical analyses were performed using *JMP v. 14.0.0* (JMP, 2018).

The drivers for hydrological and soil performance metrics were quantified with a two-step linear regression analysis. In the first step, the correlation of performance with each external driver (i.e., inflow rate, antecedent degree of saturation, surface and soil temperature, and snow depth) was considered. The drivers that had the highest correlation and level of significance were determined as primary drivers. In the second step, a multiple linear regression analysis was conducted first with the primary drivers. Single and multiple linear regression analyses were performed for the performance metrics using performance indicators such as inflow rate, surface and soil temperature, degree of saturation, and snow depth by adding one indicator at a time to each model. For each performance indicator the model with the best coefficient of determination was chosen. Parameters that did not enhance the model performance were eliminated from the analysis.

3. Results

3.1. Continuous monitoring results

The winter and spring 2019-2020 monitoring period was representative of average climatic conditions in Reykjavík (Arnardottir, 2020): (1) 457 mm of precipitation fell during the six months starting in November; (2) Intermittent snow cover, with 12 snow cycles lasting from 1 to 25 days (Fig. 4a); (3) 21 days of sub-zero average air temperature, the longest cycle lasting for 10 consecutive days (Fig. 4b); (4) 15 soil

freeze-thaw cycles, the longest period with sub-zero soil temperature lasted for 15 consecutive days (Fig. 4c). The maximum daily snow depth from Reykjavik Station No.1 was 12 cm, which was approximately half of the range measured in the study swale as the swale can accumulate more snow. During this period, the soil water content remained relatively constant at field capacity at each depth (Fig. 4 d). Soil infiltration was noted by the momentary increases in water content at all depths during rain, RoS, and synthetic runoff experiments. Conversely, frost formation was reflected by the reduction in the measured soil water content at 5 cm depth corresponding to the phase change from liquid to solid. The presence of surface frost was identified when the soil moisture content at 5 cm depth did not reach full saturation during the synthetic experiments and/or when soil temperature was below 0 °C prior to the experiment. The most prolonged period of surface frost lasted from February 9 until March 29, 2020 (Fig. 4c and d; shaded area). The runoff experiments (dotted vertical lines; Fig. 4c and d) were timed to capture the range of the experimental conditions, i.e., frost and snow.

3.2. Swale performance indicators

The synthetic runoff experiments in the grass swale highlight hydrological impairment in winter, especially during frost (F) and snow on frost (SoF). With the exception of areal efficiency (*AE*), all performance metrics were statistically lower in presence of frost than when compared to warm ground conditions (Table 3; Fig. 5). Peak flow reduction dropped by a factor of 2.1 and 3.5, and volume reduction by a factor of 1.9 and 2.5 during frost in relation to neutral and warm conditions, respectively (Fig. 5a and b). Similarly, the outflow lag time (T_{lag}), representative of swale residence

time, was 2.1 to 3.6 times lower during frost (F). This is consistent with the lower infiltration capacity and surface roughness of the grass cover. The drainage capacity (*DC*) was lowest in the presence of frost (SoF and to a lesser extent F; Fig. 5e). Although the average results for frost conditions were similar for the performance metrics tested (first two columns, Table 3), a greater variance was observed during F than SoF. Specifically, it should be noted that the maximum drainage capacity during frost matched the maximum during the warm period, which suggests that the type of frost or the extent to which the soil was frozen differed considerably.

A large variance was noted in the experimental runs during snow only conditions (S) suggesting that not only snow presence, but also snow characteristics such as depth and density, were influential factors. But on average, volume reduction was significantly higher in the presence of snow compared to frozen conditions (Table 3; Fig. 5b), indicating that a portion of the runoff volume was stored in the snowpack and was not released as outflow. The lag time was also longer, which can be explained by the initial wetting phase being longer in the presence of the snow (Fig. 5c; Fig. 3b). The *AE*, however, was on average lower during snow than frost conditions (Fig. 5d), consistent with the visual observation of the concentration of surface runoff (Fig. 3c).

The relative influence of surface versus soil conditions on the four hydrologic performance metrics was assessed by considering relationships with external experimental parameters. A single linear regression relationship, SLR, was performed to identify the key external drivers (i.e., inflow rate, antecedent moisture content, temperature, and snow depth), followed by a multiple linear regression analysis, MLR, to assess the relative importance of the top three to four co-acting drivers. Both single

and multi-regression analyses highlighted the hydraulic loading (presented as inflow rate, Q_{in}) and surface temperature as the primary performance drivers for the event-based performance metrics, followed by initial snow depth (Table 4). Because of the considerable intercorrelation between surface temperature and soil temperature, only the parameter with higher correlation was incorporated in the multi-regression models.

The MLR confirmed that higher hydraulic loading reduced the flow attenuation, on the one hand, while increasing *AE* on the other hand (note signs in Table 4). Low surface and soil temperatures and high snow depth reduced the performance. These three external drivers accounted for 68% and 57% of the natural variance of flow and volume reduction, and 51% for *AE*. T_{lag} was largely governed by the inflow rate and snow depth which contributed to delayed outflows. Surface temperature was not significantly correlated with T_{lag} in the SLR but was significant in the overall MLR model. The initial degree of saturation was not significant but did enhance the MLR model. *DC* differed vastly from the other performance metrics by being neither affected by surface conditions nor hydraulic loading (not shown, Table 4). Instead, the degree of saturation 24 hours after the event was found to be mostly regulated by the maximum degree of saturation, DS_{max}, which was attained during the event, as well as the 24-hour average soil temperature. These two soil-related parameters accounted for 64% of the variance.

Peak flow reduction was a measure of the steady state abstraction due to infiltration during the experiments using the constant flow rates in this study. Upon reaching steady state, infiltration volume becomes independent of inflow rate. Hence, the flow attenuation decreased with the increase in inflow rate. This relationship was strongest in neutral winter conditions ($R^2 = 0.65$, $p < 0.01$; Fig. 6a). In snow conditions, the

379 underlying soil was similar in nature to neutral conditions and consequently the
380 relationship was just as strong (Fig. 6b). But as snow reduced *AE*, the flow and volume
381 attenuation were lower than in neutral conditions. In the presence of frost (F and SoF),
382 the relationship was less strong and more variations in infiltration capacity were
383 observed (Fig. 6c and d; left panel). In frost only conditions, the relationship between
384 inflow rate and *AE* was stronger than when snow was present on top of frost as
385 expected (Fig. 6c and d; right panel). In warm conditions, however, the relationship
386 between inflow rate and flow attenuation broke down (Fig. 6e). This suggests that
387 another factor was influencing peak flow reduction, i.e., the initial degree of soil
388 saturation, which, as previously mentioned, did not significantly influence the hydrologic
389 performance metrics over the entire season ($p > 0.05$, Table 4). Nevertheless, the
390 antecedent degree of saturation was found to be a major driver explaining the variability
391 in flow attenuation in summer, albeit not statistically significant at the 5% level (Fig. 7).
392 In winter, the degree of saturation did not exert a significant influence on peak flow
393 reduction.
394
395 3.3. Hydrologic response of the swale
396 No significant correlation was found between hydrological performance of the swale
397 and either snow depth or the initial degree of saturation over the entire study period
398 (Table 4). However, a closer look at specific runoff experiments provides valuable
399 insights into the processes that were not fully explained by statistical significance tests.
400 To better understand the relationship between the hydrological response and the initial
401 degree of saturation, the hydrographs of two consecutive experiments in summer 2019

402 were considered (Fig. 8a and b). Preceded by an abnormally long dry period of 2
403 weeks, the initial degree of saturation was at an absolute seasonal low (50%) prior to
404 the former, medium flow experiment. The corresponding peak flow and volume
405 reductions were the highest recorded throughout the study period for a medium flow (61
406 and 75%, respectively). The initial degree of saturation was much higher in the
407 consecutive experiment (70%). A higher outflow rate was observed in the second
408 experiment despite the much lower inflow rate used. Consequently, flow and volume
409 reductions were reduced by a factor of 2 due to the increase in the initial water content
410 (Fig. 8b).

411 Regression analyses indicated a negative relationship between snow depth and the
412 swale performance metrics (Table 4), though not statistically significant. This confirmed
413 that runoff events became more voluminous with the addition of meltwater. But this
414 result is not generalizable, as noted from the hydrographs during two runoff experiments
415 with 30 cm thick snow cover (Fig. 8c and d). When the soil was frozen and a high inflow
416 rate was used, the water was initially stored in the snow to be suddenly released
417 afterwards in a dam-burst- like manner, producing an outflow peak that exceeded the
418 inflow rate. However, volume reduction was 23% due to the storage of runoff water in
419 the snowpack. In contrast, when the soil was not frozen and a low inflow rate was used,
420 the delay in outflow was 24 minutes which is the longest T_{lag} observed during the study
421 period. The runoff peak did not surpass the inflow rate and the volume reduction was as
422 high as 83%. This indicated that the presence of thick snow cover can either accentuate
423 or severely attenuate runoff peaks, while providing considerable volume reduction.
424

3.4. Soil response during winter runoff events

Long-term measurements of soil and hydrological inputs provide valuable insights into the influential factors that contributed to frost formation. The first surface frost occurred after a rainfall event on November 22 (Fig. 4b; double dashed line) that was followed by a freezing cycle (min. -8.3 °C). The second soil frost period occurred in December due to a long period of surface cooling. The soil thawed in January, during which time the water content at 5 cm repeatedly peaked at 54% (corresponding to 99% degree of saturation). Two synthetic experiments on January 29 and 31 accompanied with subfreezing air temperature (min. -6.4 °C), led to frost formation at the 5 cm soil horizon, during this period the soil temperature dropped to a minimum of -1.3 °C. Frost was interrupted once again on February 7 as a result of a RoS event accompanied by an increase in air temperature (max. 8.1 °C). Following that, a sharp reduction in temperature was recorded (min. -10 °C), and with the absence of an insulating snow cover, surface water content dropped dramatically to 7%. These frost conditions were maintained for almost one and a half months, which was reflected in both an uncharacteristically low water content and limited response at 5 cm soil depth during the subsequent runoff events. The successive wetting of the soil during this period resulting from the multiple snowmelt events, as well as the synthetic runoff experiments led to the extended period of frozen soil which lasted until the end of winter.

A closer look at the changes in soil saturation and temperature during specific events gives insights into the variations in frost type and infiltration capacity. When the soil was partially frozen (Fig. 9a; left panel), the water content in the deeper layers responded almost immediately to hydrological inputs while the top layer responded

448 gradually peaking at 14% saturation at the end of the experiment . Hence, pore ice was
449 present in the top 5 cm throughout the experiment, while, at the same time, allowing
450 water to seep to the non-frozen ground below. Moreover, infiltrating water melted some
451 of the frost in the topsoil during the experiment. This suggests that preferential flow
452 paths and/or air-filled pores were present within the top frozen layer. During the most
453 severe frost event (February 17; Fig. 9a; center), the deeper layers of the soil also
454 responded to the runoff at the surface. However, the response was slightly delayed
455 indicative of more resistance to the flow which might have resulted from frost
456 penetration within the 5-15 cm soil horizon and thereafter thawing with the infiltrating
457 water (Fig. 9a and b; center). It should be noted that the topsoil was frozen throughout
458 the inflow period (i.e., soil saturation remained at 6%). In spite of this, downward water
459 movement was still observed in the swale media. By the end of April (Fig. 9a; right), the
460 soil returned to neutral conditions, as attested by the increase in saturation in the entire
461 soil profile during the experiment on April 30. Lastly, the seasonal variations in soil
462 porosity of the top layer throughout the study period showed two interrupted periods of
463 low porosity. The first of these was during experiments in November and December and
464 the second during experiments in February and March (Fig. 9c). Afterwards, the
465 topsoil's porosity increased from 87% on April 8 to 98% on April 30 when the soil
466 thawed completely. This suggested that the swale did not undergo a consistent
467 reduction in infiltration capacity during winter but was subjected to repeated cycles of
468 freezing and thawing as a result of the frequent rainfall events accompanied with an
469 increase in air temperatures.
470

4. Discussion

4.1. Seasonal swale performance in cold maritime climate

The focus of this research was on the winter performance of grass swales, which are usually designed to infiltrate and treat small rainfall events and attenuate peak flow from large events (Woods Ballard et al., 2015). The 5.8 m long test section of the swale infiltrated on average 46% of the low flow rates (0.65-1 l/s) during the study period, which covered winter, spring, and summer. These low hydraulic loadings constituted almost half of the measured flows naturally entering the SuDS system. The infiltration was, on average, 7% and 32% for the higher flowrates during winter and summer, respectively. During extreme frozen conditions, a significant reduction in infiltration capacity was observed. Nevertheless, there were no indications that the swale capacity was exceeded. Overflowing of the side slopes was never observed in the swale, and the average flow depth was kept below 10 cm.

The winter hydrological performance decline observed in this study was consistent with previous research connecting reduced winter performance with vegetation dormancy and lower temperatures (Roseen et al., 2009). But more importantly, this study showed that the winter performance in a cold maritime climate fluctuated on a synoptic basis because of intermittent frost formation at the surface, and to a lesser extent, frequent snow cycles. The results of this study are best compared with SuDS studies in cold coastal regions experiencing frequent freeze-thaw and RoS events, namely in the prairie environments in Canada and in Norway. Khan et al. (2012) observed an average peak flow reduction in bioretention cells of 92% for winter events with hydraulic loading of 25 cm/h. This was attributed to the water eventually infiltrating

via preferential flow paths and reaching the underdrain without utilizing the entire media despite the presence of frost at a depth of 15 cm. Similarly, Paus et al. (2015) found that the total volume reduction achieved by three bioretention cells ranged between 55 to 100%. In contrast, the average flow attenuation in the swale in this study was only 13% for hydraulic loadings ranging between 19 to 131 cm/h. This comparison supports the findings of Roseen et al. (2009) that swales suffer the most noticeable performance decline in winter of SuDS elements. This can be attributed to the shorter retention time in a conveyance-based system such as swales compared to retention-based systems such as bioretention cells.

4.2. The interactions between runoff, snow, and soil frost

Muthanna et al. (2008) hypothesized that RoS played a role in frost formation based on the observation that the infiltrated stormwater refroze following both RoS and rainfall events. Roseen et al. (2009) also noted that frost resulting from freeze-thaw cycles was common and that soil freezing usually occurred before and after rain and snowmelt events. However, neither study quantified the effects of the frequent freeze-thaw cycles, the interactions between snow and frost, or their impact on subsequent events. In this study, however, synthetic runoff events were conducted in the presence of snow with the intention to simulate RoS events. Closely spaced water content and temperature measurements at different soil depths allowed for a continuous assessment of soil infiltration and frost formation in grass swales over an entire winter. The results clearly demonstrate that intermittent midwinter rain and RoS events led to high water contents and promoted frost formation. Specifically, during winter 19/20, three events (natural

517 and synthetic) initiated separate freezing cycles which reduced soil porosity (Fig. 4c and
518 d). The temporal wetting of the soil, which in some cases was combined with the
519 removal of the snow cover, rendered the soil more susceptible to temperature
520 fluctuations, as evidenced in the sharp reduction in soil temperature following these
521 events (Fig. 4c). This is a common complication with the implementation of SuDS in
522 coastal cold regions that experience repeated RoS and freeze-thaw cycles (Khan et al.,
523 2012; Muthanna et al., 2008).
524

525 4.3. Key mechanisms affecting winter infiltration

526 The primary mechanism for hydrological performance deterioration was soil frost.
527 Soil permeability in the presence of frost varied across experiments due to the
528 heterogeneous nature of soils and frost formation, as well as the presence of cracks
529 and preferential flow paths resulting from the frequent freeze-thaw cycles. Spatial
530 variability was observed in six single-ring infiltration measurements conducted in an
531 adjacent swale (Zaqout, unpublished data). On any given day, infiltration was impeded
532 in certain locations while it was not affected in other locations. The formation of porous
533 or granular frost with loose ice crystals may permit or even enhance infiltration
534 (Flerchinger et al., 2013). A common factor that influences infiltration is frost depth
535 (Fach et al., 2011). In this study, frost was only detected in the topmost layer at 5 cm
536 soil depth (Fig. 4c and d). It is not clear how far the frost penetrated between 5 and 15
537 cm depth. Soil temperature at 5 cm intervals within the first 20 cm of the profile would
538 have helped clearing this ambiguity on maximum frost depth. However, an excellent

indication of soil infiltration and frost formation throughout the soil matrix was provided by water content probes spaced 10 cm apart (see Fig. 9 and discussion thereof).

The secondary mechanism that negatively affected winter performance was snow cover. Snow reduced the swale's surface area by concentrating surface runoff which would have otherwise been more evenly distributed in snow-free conditions. Moreover, the added snowmelt led to more voluminous runoff events and reduced water temperature, which negatively affects infiltration. Nevertheless, for the least intense runoff experiments (low flow), snow was also found to enhance the hydrological performance by storing significant amounts of runoff water and by delaying flow peaks. This storage function was dependent, however, on snow properties and the underlying soil conditions. Water stored in the snowpack was released instantaneously in a "dam-burst-like" release of water when thick snow was coupled with the presence of soil frost or dense snow layers. Such a burst was only observed once in this study, making further investigations necessary to verify the results. Lastly, the storage function of the snow becomes less important in longer duration events, as all of the snow will melt eventually and add to runoff. Most of the extreme winter flooding events recorded in Reykjavík involved more than 6 hours of rainfall (Arnardottir, 2020).

4.4. The importance of soil drainage in design

Previous studies have found that initial degree of saturation negatively influences the hydrological performance of SuDS (Rujner et al., 2018). This relationship was only detected during summer in this study, after dry periods lasting for weeks at a time (Fig. 7). Degree of saturation is highly linked with *DC*: Poorly drained soils tend to maintain a

562 high degree of saturation, which in turn reduces their capacity to mitigate subsequent
563 events. A *DC* in the range of only 20 to 26%, as in this study, might have exacerbated
564 the impacts of winter conditions and promoted frost formation. Additionally, the high
565 water content in the swale also affected the performance during non-frozen conditions
566 by reducing the available volume for infiltration at the onset of runoff events. This was
567 consistent with the previous findings from studies on infiltration-based systems (e.g.,
568 LeFevre et al., 2009; Muthanna et al., 2008) and emphasizes the importance of proper
569 soil drainage, especially for winter operations.

570 We argue that *DC* is particularly important in a cold maritime climate, which
571 frequently experiences precipitation in liquid form (as opposed to solely dry snow). The
572 combination of liquid inputs and poor *DC* makes the soils more susceptible to freezing,
573 even though air temperatures fluctuate only moderately around zero (the minimum daily
574 temperature recorded in Reykjavík is -12°C). Frost events particularly occurred 1-2 days
575 following rainfall, simulated runoff, and RoS events which might not have been a long
576 enough period to properly drain the swale media prior to the onset of freezing air
577 temperatures. This was observed in the sharp drops in moisture content and soil
578 temperature at 5 cm depth after the November 22, January 29 and 31, February 11 and
579 25, March 6 and 11 events (Fig. 4c and d). Frost formation was confirmed in the runoff
580 experiments following those events and it was reflected in the deterioration in
581 performance indicators.

582 To maintain a good soil drainage, and reduce the risk of frost formation, care must
583 be taken in the design and operation of swales. Fine-textured soils such as clay and silt
584 should be avoided in the filter media due to their low infiltration capacity and high water

holding potential. Dust accumulation might occur when swales are located next to roads or parking lots with heavy traffic, especially in cold climates where studded tires that increase road erosion are used extensively (Barr, 2020). Filter strips are often used to capture road dust and sediments before entering the swale. In this study, the swale was adhering to best practices, but the swale filtering media laid on hard compacted clay. This might explain the low drainage capacity observed throughout the study period.

5. Conclusions

Maritime winter climate is both wet and mild, with air temperatures fluctuating around the freezing point and precipitation falling as rainfall, rain-on-snow and snow. This research assesses the impacts of co-acting winter conditions on the hydrological performance of grass swales. To that goal, 63 synthetic runoff experiments were performed in a grass swale over 18 months. The swale hydrological performance was evaluated based on five metrics: the relative peak flow reduction, the relative infiltrated volume, runoff lag time, soil drainage capacity, and areal efficiency.

Results indicated a significant impairment in the hydrologic performance during winter. Peak flow attenuation was 13% in winter as compared to 20-40% in spring and summer. Similarly, the relative infiltrated volume was 22% in winter vs. 30-60% during the warm season. Poor flow attenuation was primarily associated with the reduction in soil porosity in the top 5 cm horizon because of the formation of ice lenses. However, macropores created by vegetation roots, biological activity, and the frequent freeze-thaw cycles allowed for infiltration to the deeper layers of the soil. Thus, no concrete frost fully blocking infiltration was observed during the study period. Runoff lag times

where three times shorter in winter compared to summer reflecting a reduction in surface roughness. While the surface frost significantly reduced the overall performance of the swale, it did not compromise the swale overall function of attenuating small and medium events.

Snow cover provided both initial storage and resistance to overland flow resulting in longer lag times and high volume reduction during short-duration, low hydraulic loading events. But as an event progressed, overland flow formed in a concentrated path within the snowpack, effectively reducing the area of infiltration. The snow melted and added to the runoff volume. In the most severe case, the runoff initially stored in a thick snow was released instantaneously similar to a dam burst to the effect that the outflow exceeded inflow the swale. Hence, the combination of sudden snowmelt and low infiltration capacity can generate more intense rain-on-snow induced runoff events. However, this condition was observed only once in this study.

This study provided, to the authors' best knowledge, the first systematic assessment of the relative importance of hydraulic loading, surface and soil conditions on the seasonal performance of grassed swales in a cold climate. Single and multivariate regression analyses highlight that winter peak flow and volume reduction were primarily affected by surface temperature, followed by hydraulic loading and to a lesser extent snow depth. The conditions of the underlying soil did not significantly affect the infiltration in winter but played a large role in explaining the variance in summer performance. The highest infiltration capacity observed in this study was when the soil was half saturated, which occurred in summer following a two-week dry period. Runoff lag times and areal efficiency were primarily affected by inflow rate and

631 secondarily by surface conditions, such as snow depth. Soil drainage capacity was,
632 however, governed by the 24-hour average swale media temperature following the
633 event and the maximum soil saturation reached during the event.

634 In a maritime climate, with air temperature oscillating in the order of 15 times around
635 the freezing point during winter, precipitation falls often in liquid form. Frequent rain and
636 rain-on-snow infiltrates the ground which keeps the soil moist. In the absence of an
637 insulating snow cover, the soil is more susceptible to freezing. Frost was observed to
638 form within 1-2 days after runoff events, which negatively affected the swale's ability to
639 infiltrate subsequent events. This combined with a soil drainage capacity of only 20-26%
640 in 24 hours, as found in this study, kept the soil highly saturated during winter and more
641 susceptible to freezing.

642 With rising winter temperatures, regions that historically underwent a seasonal frost
643 and snow period may now experience more frequent and intense mid-winter rain-on-
644 snow followed by frost. This study confirms that SuDS may serve as a low impact, low-
645 cost solution to reduce urban flooding in such cyclic climatic winter conditions. A special
646 attention is, however, required in the design and operation of SuDS in relation to rain-
647 on-snow and frost cycles. Proper soil drainage is instrumental in order to maintain the
648 soil relatively dry and less susceptible to the frequent freezing. Limiting the presence of
649 fine sediments that decrease infiltration is required both in the filter media during the
650 construction phase and from surface loading during the operation lifetime of swales.
651 The reduction in infiltration capacity during winter must also be taken into account when
652 sizing SuDS. Therefore, incorporating site-specific considerations is recommended for
653 the designing of infiltration-based components.

654

655 **Acknowledgements**

656 This research was funded by the Icelandic Research Fund (Icelandic: Rannís), grant
657 number 185398-053. We thank the Gardabaer Municipality, Iceland Meteorological
658 Office, in particular, for operating the Urridaholt weather station; Urridaholt ehf, the
659 Department of Water Supply in Gardabaer, and the Fire Department in Hafnarfjörður for
660 the help with running the field program. We also thank Halldóra Hreggvidsdottir for her
661 instrumental help with starting this research project. We are also grateful to Guðni
662 Þorvaldsson and Berglind Orradottir at The Agricultural University of Iceland for their
663 help in setting up the soil monitoring program. A special thanks goes to our technician
664 Vilhjálmur Sigurjónsson for his help with the experimental setup. The authors also thank
665 the four anonymous reviewers for their thoughtful feedback on the manuscript.

References

Abu-Zreig, M., Rudra, R. P., Lalonde, M. N., Whiteley, H. R., & Kaushik, N. K. (2004). Experimental investigation of runoff reduction and sediment removal by vegetated filter strips. *Hydrological Processes*, *18*(11), 2029–2037. https://doi.org/10.1002/hyp.1400

Ahmed, F., Gulliver, J. S., & Nieber, J. L. (2015). Field infiltration measurements in grassed roadside drainage ditches: Spatial and temporal variability. *Journal of Hydrology*, *530*, 604–611. https://doi.org/10.1016/j.jhydrol.2015.10.012

Arnardóttir, A. R. (2020). *Winter Floods in Reykjavík: Coaction of Meteorological and Soil Conditions*. Master thesis.

ASTM. (2009). *D7263, Standard Test Methods for Laboratory Determination of Density (Unit Weight) of Soil Specimens*. ASTM International, West Conshohocken, PA. https://www.astm.org/Standards/D7263.htm

ASTM. (2017). *D6913, Standard Test Methods for Particle-Size Distribution (Gradation) of Soils Using Sieve Analysis*. ASTM International, West Conshohocken, PA. https://www.astm.org/Standards/D6913.htm

ASTM. (2019). *D2434, Standard Test Method for Permeability of Granular Soils (Constant Head).* ASTM International, West Conshohocken, PA. https://www.astm.org/Standards/D2434.htm

685 Bäckström, M., & Viklander, M. (2000). Integrated stormwater management in cold
686 climates. *Journal of Environmental Science and Health, Part A*, *35*(8), 1237–1249.
687 https://doi.org/10.1080/10934520009377033

688 Barr, B. (2020). *Processes and Modeling of Non-Exhaust Vehicular Emissions in the*
689 *Icelandic Capital Region.* Master thesis.

690 Blecken, G.-T., Zinger, Y., Muthanna, T. M., Deletic, A., Fletcher, T. D., & Viklander, M.
691 (2007). The influence of temperature on nutrient treatment efficiency in stormwater
692 biofilter systems. *Water Science and Technology: A Journal of the International*
693 *Association on Water Pollution Research*, *56*(10), 83–91.
694 https://doi.org/10.2166/wst.2007.749

695 Caldwell, T. G., Bongiovanni, T., Cosh, M. H., Halley, C., & Young, M. H. (2018). Field
696 and Laboratory Evaluation of the CS655 Soil Water Content Sensor. *Vadose Zone*
697 *Journal*, *17*(1), 0. https://doi.org/10.2136/vzj2017.12.0214

698 Davis, A. P., Stagge, J. H., Jamil, E., & Kim, H. (2012). Hydraulic performance of grass
699 swales for managing highway runoff. *Water Research*, *46*(20), 6775–6786.
700 https://doi.org/10.1016/j.watres.2011.10.017

701 Deletic, A., & Fletcher, T. D. (2006). Performance of grass filters used for stormwater
702 treatment—A field and modelling study. *Journal of Hydrology*, *317*(3–4), 261–275.
703 https://doi.org/10.1016/j.jhydrol.2005.05.021

704 Dietz, M. E., & Clausen, J. C. (2008). Stormwater runoff and export changes with
705 development in a traditional and low impact subdivision. *Journal of Environmental*
706 *Management*, *87*(4), 560–566. https://doi.org/10.1016/j.jenvman.2007.03.026

Dong, C., & Menzel, L. (2020). Recent snow cover changes over central European low mountain ranges. *Hydrological Processes*, *34*(2), 321–338. https://doi.org/10.1002/hyp.13586

Fach, S., Engelhard, C., Wittke, N., & Rauch, W. (2011). Performance of infiltration swales with regard to operation in winter times in an Alpine region. *Water Science and Technology*, *63*(11), 2658–2665. https://doi.org/10.2166/wst.2011.153

Flerchinger, G. N., Lehrsch, G. A., & McCool, D. K. (2013). Freezing and Thawing | Processes. In *Reference Module in Earth Systems and Environmental Sciences* (p. B9780124095489053000). Elsevier. https://doi.org/10.1016/B978-0-12-409548-9.05173-3

García-Serrana, M., Gulliver, J. S., & Nieber, J. L. (2017). Infiltration capacity of roadside filter strips with non-uniform overland flow. *Journal of Hydrology*, *545*, 451–462. https://doi.org/10.1016/j.jhydrol.2016.12.031

Garvelmann, J., Pohl, S., & Weiler, M. (2015). Spatio-temporal controls of snowmelt and runoff generation during rain-on-snow events in a mid-latitude mountain catchment. *Hydrological Processes*, *29*(17), 3649–3664. https://doi.org/10.1002/hyp.10460

Gavrić, S., Leonhardt, G., Marsalek, J., & Viklander, M. (2019). Processes improving urban stormwater quality in grass swales and filter strips: A review of research findings. *Science of The Total Environment*, *669*, 431–447. https://doi.org/10.1016/j.scitotenv.2019.03.072

727 Khan, U. T., Valeo, C., Chu, A., & van Duin, B. (2012). Bioretention cell efficacy in cold
728 climates: Part 1 — hydrologic performance. *Canadian Journal of Civil Engineering*,
729 *39*(11), 1210–1221. https://doi.org/10.1139/l2012-110

730 Iceland Meteorological Office [IMO] (2020a). *Ten-minute Weather and Rainfall Data at*
731 *Gardabaer, Urridaholt Station No. 1474.* Data delivery April 21, 2020.

732 Iceland Meteorological Office [IMO] (2020b). *Daily Snow Depth at Reykjavík Manned*
733 *Synoptic Station No. 1.*

734 LeFevre, N. J., Davidson, J. D., & Oberts, G. L. (2009). Bioretention of Simulated
735 Snowmelt: Cold Climate Performance and Design Criteria. *Cold Regions*
736 *Engineering 2009*, 145–154. https://doi.org/10.1061/41072(359)17

737 Liu, Y.-J., Hu, J.-M., Wang, T.-W., Cai, C.-F., Li, Z.-X., & Zhang, Y. (2016). Effects of
738 vegetation cover and road-concentrated flow on hillslope erosion in rainfall and
739 scouring simulation tests in the Three Gorges Reservoir Area, China. *CATENA*,
740 *136*, 108–117. https://doi.org/10.1016/j.catena.2015.06.006

741 Moghadas, S., Leonhardt, G., Marsalek, J., & Viklander, M. (2018). Modeling Urban
742 Runoff from Rain-on-Snow Events with the U.S. EPA SWMM Model for Current and
743 Future Climate Scenarios. *Journal of Cold Regions Engineering*, *32*(1), 04017021.
744 https://doi.org/10.1061/(ASCE)CR.1943-5495.0000147

745 Monrabal-Martinez, C., Aberle, J., Muthanna, T. M., & Orts-Zamorano, M. (2018).
746 Hydrological benefits of filtering swales for metal removal. *Water Research*, *145*,
747 509–517. https://doi.org/10.1016/j.watres.2018.08.051

748 Muthanna, T. M., Viklander, M., & Thorolfsson, S. T. (2008). Seasonal climatic effects
749 on the hydrology of a rain garden. *Hydrological Processes*, *22*(11), 1640–1649.
750 https://doi.org/10.1002/hyp.6732

751 Orradottir, B., Archer, S. R., Arnalds, O., Wilding, L. P., & Thurow, T. L. (2008).
752 Infiltration in Icelandic Andisols: The Role of Vegetation and Soil Frost. *Arctic,*
753 *Antarctic, and Alpine Research*, *40*(2), 412–421. https://doi.org/10.1657/1523-
754 0430(06-076)[ORRADOTTIR]2.0.CO;2

755 Paus, K. H., Muthanna, T. M., & Braskerud, B. C. (2015). The hydrological performance
756 of bioretention cells in regions with cold climates: Seasonal variation and
757 implications for design. *Hydrology Research*, nh2015084.
758 https://doi.org/10.2166/nh.2015.084

759 Roseen, R. M., Ballestero, T. P., Houle, J. J., Avellaneda, P., Briggs, J., Fowler, G., &
760 Wildey, R. (2009). Seasonal Performance Variations for Storm-Water Management
761 Systems in Cold Climate Conditions. *Journal of Environmental Engineering*, *135*(3),
762 128–137. https://doi.org/10.1061/(ASCE)0733-9372(2009)135:3(128)

763 Rujner, H., Leonhardt, G., Marsalek, J., Perttu, A.-M., & Viklander, M. (2018). The
764 effects of initial soil moisture conditions on swale flow hydrographs. *Hydrological*
765 *Processes*, *32*(5), 644–654. https://doi.org/10.1002/hyp.11446

766 Shafique, M., Kim, R., & Kyung-Ho, K. (2018). Evaluating the Capability of Grass Swale
767 for the Rainfall Runoff Reduction from an Urban Parking Lot, Seoul, Korea.
768 *International Journal of Environmental Research and Public Health*, *15*(3), 537.
769 https://doi.org/10.3390/ijerph15030537

770 Shen, J. (1981). *Discharge Characteristics of Triangular-notch Thin-plate Weirs*. United
771 States Department of the Interior, Geological Survey.

772 USDA. (1987). Soil Mechanics Level 1: Module 3—USDA Textural Soil Classification.
773 *Study Guide*.

774 Valeo, C., & Ho, C. L. I. (2004). Modelling urban snowmelt runoff. *Journal of Hydrology*,
775 *299*(3), 237–251. https://doi.org/10.1016/j.jhydrol.2004.08.007

776 Viessman, W., & Lewis, G. L. (2002). *Introduction to Hydrology 5th edition*. Prentice
777 Hall.

778 Woods Ballard, B., Wilson, S., Udale-Clarke, H., Illman, S., Scott, T., Ashley, R., &
779 Kellagher, R. (2015). *The SUDS manual (C753). CIRIA: London, UK.* ISBN 978-0-
780 86017-759-3

781 **Tables**

782 Table 1 Summary of soil characteristics determined in the laboratory using samples extracted
783 from the study swale.

Soil characteristics	
Soil texture	Sandy loam
Gravel: sand: fines	15-20:75-82:2.5-4
Bulk density (ρ_s)	1.2-1.42
Porosity (ϕ)	0.46-0.53
Organic content	2-8%
Saturated hydraulic conductivity (K_{sat})	6.23 ($\pm$ 0.10) × 10^{-5} m/s

785 Table 2 Range of experimental initial conditions during the period of spring 2019 to summer
786 2020.

	DS_{ini} (%)	T_{air} (°C)	T_{surf} (°C)	Q_{in} (l/s)	SD (cm)
Average:	70	6.1	5.6	2.0	17.5
Range:	49-90	-3 to 19	-1 to 20	Very low: 0.2 Low: 0.65 to 1.0 Medium: 2 ± 0.2 High: 4.2 ± 0.3	2 to 30

Notes: Q_{in} = inflow rate; DS_{ini} = initial degree of saturation; T_{air} = air temperature; T_{surf} = soil surface temperature; SD = snow depth.

788 Table 3 Means (standard deviations) of the hydrological performance metrics for the different
789 surface conditions and the level of significance for the comparison between the specific winter
790 conditions i.e., frost (F), snow on frost (SoF), and snow (S) and neutral (N) and warm (W)
791 conditions.

	Winter			**Reference**	
	F	SoF	S	N	W
	(*n* = 10)	(*n* = 9)	(*n* = 7)	(*n* = 9)	(*n* = 24)
$\Delta Q_{pk\ rel}$	12 (7.3)	11 (3.6)	16 (8.5)	25 (8.0)	38 (10)
	/*	**/***	+/***	-	-
$\Delta V_{inf\ rel}$	19 (11)	20 (8.5)	39 (26)	37 (11)	50 (14)
	/*	*/***	+/+	-	-
T_{lag}	1.6 (0.8)	2.3 (1.2)	7.4 (8.0)	3.3 (2.2)	5.7(3.0)
	+/**	+/*	*/+	-	-
AE	58 (11)	53 (8.6)	43 (16)	58 (11)	63(11)
	+/+	+/*	*/***	-	-
DC	21(5.3)	20 (0.8)	23 (3.3)	22 (3.0)	26(1.5)
	+/*	+/***	+/+	-	-

Notes: Significance in relation to N/W. $^{+}$ $p > 0.05$ * $p < 0.05$ ** $p < 0.01$ *** $p < 0.001$.

793 Table 4 Multiple and single regression for the performance metrics, regression coefficients, standards error, correlation coefficients,

794 and models R^2. Not included parameters referred to as N/I.

MODEL		$\Delta Q_{pk\ rel}$		$\Delta V_{inf\ rel}$		*AE*		T_{lag}	
		B (SE)	*r*	*B (SE)*	*r*	*B (SE)*	*r*	*B (SE)*	*r*
1	Q_{in}	-2.95 (0.77)	-0.38**	-6.61 (1.33)	-0.47***	5.82 (0.96)	0.51***	-1.50 (0.27)	0.24***
	T_{sur}	1.41 (0.17)	0.76***	1.51 (0.27)	0.62***	N/I	N/I	0.19 (0.06)	0.06^{+}
	T_{soil}	N/I	N/I	N/I	N/I	0.96 (0.25)	0.36**	N/I	N/I
	R^2	0.66***		0.53***		0.47***		0.27***	
2	DS_{ini}	N/I	N/I	-0.24 (0.18)	-0.01^{+}	N/I	N/I	-0.05 (0.04)	0.00^{+}
	SD	-0.17 (0.15)	-0.34^{+}	0.38 (0.25)	-0.07^{+}	-0.37 (0.19)	-0.28^{+}	0.27 (0.05)	0.17**
	R^2	0.68***		0.57***		0.51***		0.58***	

Notes: B = regression coefficient for MLR. SE = std. error. r = correlation coefficient for SLR. $^{+}$ $p > 0.05$ * $p < 0.05$ ** $p < 0.01$ *** $p < 0.001$. T_{sur} = surface temperature. T_{soil} = avg. soil temperature 5-45 cm depth. DS_{ini} = initial degree of saturation. SD = snow depth.

795

Abstract

Sustainable urban drainage solutions (SuDS) are a diverse set of design options that mitigate floods and improve water quality. Grass swales are the sole component of SuDS that transports runoff over long distances to downstream recipients. A deeper understanding of the performance of grass swales in different winter conditions is important in order for cities to achieve a greater climate resiliency. The goal of this study was to assess the impacts of frequent rain-on-snow, and freeze-thaw cycles on the hydrologic performance of grass swales. A total of 63 field synthetic runoff experiments were performed in a 5.8 m long section of a grass swale in the Urriðaholt neighborhood, Gardabaer, Iceland over 18 months. A three-fold reduction in peak flow attenuation was observed in winter (avg. 13%) compared to summer (avg. 38%) for hydraulic loadings ranging between 19 to 131 cm/h. The reduction in the performance of the swale was primarily due to frost formation and secondarily due to snow. The frequent rainfall, snowmelt, and rain-on-snow events elevated the soil water content and rendered the swale media susceptible to frost formation. The formation of pore ice within the 5 cm soil horizon led to a considerable reduction in soil porosity, which negatively affected the infiltration capacity, and shortened runoff lag times. Snow affected the performance by concentrating the flow in narrow channels, which reduced the effective area of infiltration, but also led to longer lag times and stored a portion of the runoff water within its pack. Despite the deterioration in the swale efficiency in winter, infiltration was observed in all synthetic runoff experiments, indicating that frost was either porous/granular, or heterogeneous in nature. The swale served its purpose to

moderately reduce runoff peaks and volumes, especially for small and medium events. This research highlights the importance of effectively draining infiltration-based systems in cold climates to avoid the adverse effects of low temperatures.

Author contributions

Tarek Zaqout: Conceptualization, Methodology, Software, Validation, Formal analysis, Investigation, Resources, Data Curation, Writing – Original Draft, Visualization. Hrund O. Andradottir: Conceptualization, Methodology, Resources, Writing – Review and Editing, Supervision, Project administration, Funding acquisition.

Declaration of interests

☒ The authors declare that they have no known competing financial interests or personal relationships that could have appeared to influence the work reported in this paper.

☐The authors declare the following financial interests/personal relationships which may be considered as potential competing interests:

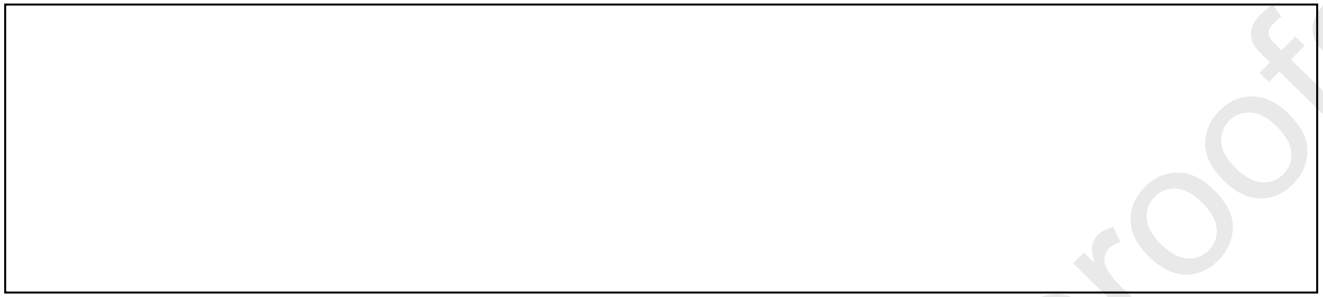

Figure

Captions

Fig. 1 Urridaholt urban catchment in Gardabær. The location of the study swale (dot), swale network (double line), the drainage area for the swale (crosshatch), building plots (even shade), streets (single heavy line), and lake Urridavatn (triangle).

Fig. 2 Schematic of the experimental setup, the swale dimensions and slopes, the location of the inflow and outflow measurements, water content and soil temperature sensors, and the delivery system.

Fig. 3 Example of synthetic experiments data collection conducted on 22.02.2020. (a) Surface hydrological response, (b) subsurface response shown as the total degree of saturation, and (c) schematic of the changes in snow cover during the experimental runs. Dotted vertical lines indicate the different phases of wetting, runoff, and drainage.

Fig. 4 Meteo-hydrological conditions during winter and spring 2019-2020. (a) Snow depth (Reykjavik Station No. 1), (b) precipitation and air temperature, (c) soil temperature, and (d) soil water content. Double dashed lines = rainfall,

synthetic experiments, and RoS events leading to frost. Dotted lines = days at which the experiments were conducted; Partial frost “PF”, no frost “NF”, and gray shade highlights the longest soil frost period.

Fig. 5 Hydrological performance metrics in terms of surface conditions. (a) Relative peak flow reduction, (b) relative volume infiltrated, (c) runoff lag time, (d) areal efficiency, and (e) soil drainage capacity.

Fig. 6 Linear regression between hydrological inputs (Q_{in}) and peak flow reduction (left) and areal efficiency (right) for different surface conditions. (a) Neutral, (b) snow, (c) snow on frost, (d) frost, and (e) warm conditions.

Fig. 7 Linear regression between the initial degree of saturation of the first events and peak flow reduction in summer (dot) and winter (triangle).

Fig. 8 Selected runoff events hydrographs. (a) Medium inflow with low degree of saturation, (b) low inflow with high degree of saturation, (c) high inflow with 30 cm of snow and frozen soil, and (d) low inflow with 30 cm of snow and unfrozen soil.

Fig. 9 Soil response during synthetic events with different soil conditions (from left to right = partially frozen, frozen, and neutral). (a) Degree of saturation, (b) soil temperature, and c) effective porosity within the first layer during synthetic experiments. Solid vertical line indicates the start of runoff.

Hydrologic performance of grass swales in cold maritime climates: Impacts of frost, rain-on-snow and snow cover on flow and volume reduction

Tarek Zaqout, Hrund Andradottir

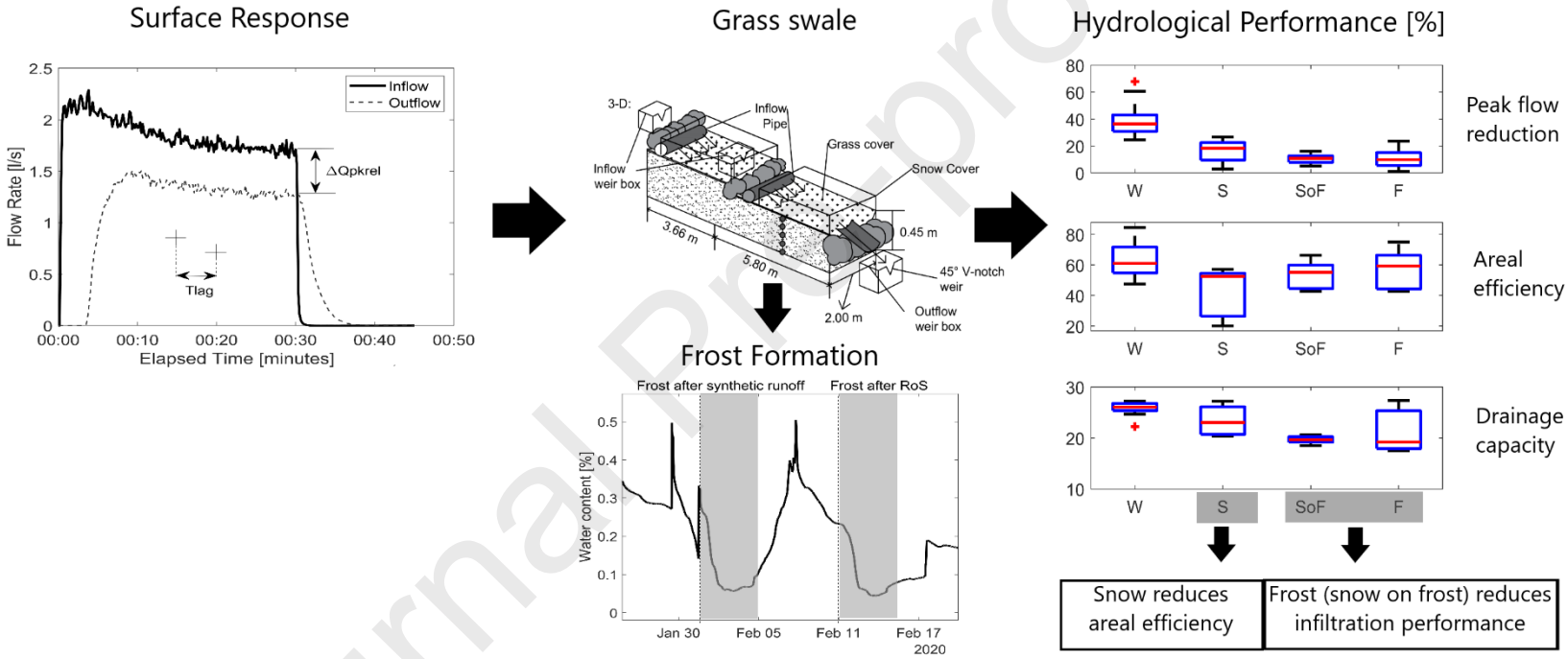

Highlights

- Swales in maritime cold climates are susceptible to frequent frost formation.

- Frost reduces soil porosity and infiltration capacity of grass swales.
- Snow leads to concentrated runoffs which reduces the infiltration capacity.
- Rain on snow events followed by freezing temperatures promote frost formation.
- A well-drained soil is essential to avoid the adverse effects of cold climates.